EAM
Environmental and Materials Journal
EAM 3(2): 145–164
ISSN 3025-0277

Institute for Advanced Science, Social and Sustainable Future
MORALITY BEFORE KNOWLEDGE

One-pot catalytic conversion of glucose to 2,5-furandicarboxylic acid over NiO-modified ZSM-5 zeolites: Effects of reaction temperature and solvent ratio

Arnia Putri Pratama[1,2], Andita Junia Mulyadi[1,2], Rahmat Wibowo[1], Yuni Krisyuningsih Krisnandi[1,2,*]

[1] *Department of Chemistry, Faculty of Mathematics and Natural Sciences, Universitas Indonesia, Depok, West Java 16424, Indonesia;*

[2] *Solid Inorganic Framework Laboratory, Department of Chemistry, Faculty of Mathematics and Natural Sciences, Universitas Indonesia, Depok, West Java 16424, Indonesia.*

*Correspondence: yuni.krisnandi@sci.ui.ac.id

Received Date: November 24, 2025 Revised Date: December 17, 2025 Accepted Date: December 31, 2025

ABSTRACT

Background: 2,5-Furandicarboxylic acid (FDCA) has gained increasing attention as a key bio-based intermediate for the production of polyethylene furanoate (PEF) and other sustainable polyesters, offering a viable alternative to fossil-derived monomers. Although FDCA is conventionally produced via oxidation of 5-hydroxymethylfurfural (HMF), direct one-pot conversion of glucose remains challenging due to the requirement for integrated catalytic functions and the strong influence of reaction conditions. Hierarchical zeolites modified with transition-metal oxides are promising for one-pot glucose-to-FDCA conversion; however, the effects of reaction temperature and solvent composition have not been systematically evaluated and are examined here using hierarchical ZSM-5, NiO-modified ZSM-5, and NiO catalysts. **Methods:** Hierarchical ZSM-5 was synthesized via a dual-template method and modified with NiO through an impregnation–spray technique to introduce redox-active sites. The catalysts were characterized using X-ray diffraction, Fourier-transform infrared spectroscopy, nitrogen physisorption, and Scanning Electron Microscope-Energy Dispersive X-Ray to establish correlations between structural, compositional, and textural properties and catalytic performance. Catalytic reactions were conducted at varying temperatures using a γ-valerolactone–water solvent system with different volume ratios. **Findings:** NiO-modified hierarchical ZSM-5 exhibited superior catalytic performance compared to the parent zeolite and NiO, achieving a maximum FDCA yield of 2.36% at 150 °C with an optimal γ-valerolactone–water ratio of 1:1. Higher FDCA yield over NiO-modified hierarchical ZSM-5 reflects the combined effects of hierarchical porosity, NiO species, reaction temperature, and solvent ratio. **Conclusion:** This study demonstrates that NiO-modified hierarchical ZSM-5 can promote one-pot glucose-to-FDCA conversion, with reaction temperature and solvent ratio identified as key parameters for performance optimization. **Novelty/Originality of this article:** This study provides a systematic assessment of the effects of reaction temperature and γ-valerolactone–water solvent ratio on FDCA formation over NiO-modified hierarchical ZSM-5 in a one-pot glucose conversion system, establishing catalyst and process design principles.

KEYWORDS: NiO; ZSM-5; NiO/ZSM-5; glucose; FDCA.

1. Introduction

The transition toward renewable carbon resources has intensified research efforts to develop sustainable chemical pathways that can replace petrochemical-based production systems (Chioatto et al., 2024). Among a wide range of value-added intermediates derived from biomass, 2,5-furandicarboxylic acid (FDCA) has emerged as a key platform molecule

Cite This Article:
Pratama, A. P., Mulyadi, A. J., Wibowo, R., & Krisnandi, Y. K. (2025). One-pot catalytic conversion of glucose to 2,5-furandicarboxylic acid over NiO-modified ZSM-5 zeolites: Effects of reaction temperature and solvent ratio. *Environmental and Materials*, *3*(2), 145-164. https://doi.org/10.61511/eam.v3i2.2025.2642

owing to its function as a precursor for polyethylene furanoate (PEF) and related furan-based polymers. These materials demonstrate enhanced gas-barrier characteristics and improved mechanical robustness relative to conventional polyethylene terephthalate (PET) (de Jong et al., 2022; Deshan et al., 2020). Establishing efficient catalytic routes for FDCA production is therefore essential to advance bio-based polymer technologies and circular carbon strategies. Glucose is an abundant, low-cost carbohydrate feedstock derived from lignocellulosic biomass, making it an attractive precursor for FDCA synthesis (Bosch & Hazen, 2013). However, the direct transformation of glucose into FDCA remains challenging because it requires a multistep cascade sequence involving isomerization, dehydration to 5-hydroxymethylfurfural (HMF), oxidation, and progressive ring functionalization (Shen et al., 2024). Each step demands specific catalytic functionalities, and integrating these steps into a single reaction environment introduces kinetic, structural, and mechanistic complexity.

Recent investigations indicate that FDCA synthesis is largely achieved by catalytic oxidation of 5-hydroxymethylfurfural (HMF), commonly facilitated by heterogeneous catalysts such as Au/C (Davis et al., 2011), Pt/CeO_2 (Gong et al., 2017), MnO_2 (Hayashi et al., 2019), and MnOx-CeO_2 (Chen et al., 2024) in the presence of molecular oxygen, peroxide, air, or $KMnO_4$ as oxidants, typically yielding 56–94% FDCA within 12–28 h under optimized conditions. Despite their encouraging catalytic performance, these systems continue to face substantial limitations in selectivity control, operational durability, and economic viability when operated under mild, environmentally sustainable conditions. From an industrial perspective, FDCA production processes are expected to achieve sufficiently high conversion efficiency and selectivity under scalable, economically feasible, and environmentally responsible conditions. Recent advances in integrated biomass valorization have sought to bypass the discrete HMF intermediate by enabling the direct conversion of carbohydrate feedstocks into FDCA via coupled dehydration–oxidation reaction sequences (Sajid et al., 2018; Tan et al., 2019). Several metal-based catalysts, such as Pd/CC (Rathod & Jadhav, 2018), Pt/C (Motagamwala et al., 2018), Au/C (Davis et al., 2011) and nano Fe_3O_4–CoO_x (Wang & Xiao, 2015) have been explored for this purpose. Nevertheless, issues such as catalyst deactivation and the high costs associated with noble metals continue to hinder broader application.

Previous studies utilized ZSM-5 derived from naturally occurring precursors and modified with CuO and NiO for the oxidative upgrading of HMF toward FDCA, achieving outstanding performance with 99.2% HMF conversion and 88.9% FDCA yield under optimal conditions of 130 °C and 11 h (Herlina et al., 2024). More recently, the production of FDCA from delignified rice husk using Ni-BTC and Cu-BTC catalysts yielded 11.7% and 10.4%, respectively, when reactions were operated at 130 °C over 9-25 h (Herlina et al., 2025). Although these findings indicate promising catalytic activity, a comprehensive systematic assessment of key reaction variables, including catalyst composition, reaction temperature, and solvent ratio, has not yet been conducted. This gap underscores the need to develop a comprehensive optimization approach that fully exploits the capabilities of these catalytic systems.

Most studies on FDCA formation have concentrated on HMF oxidation catalyzed by either homogeneous catalysts or noble-metal-supported heterogeneous materials, achieving high yields but requiring corrosive media, alkaline conditions, or expensive noble metals, which hinder broader scalability. Emerging catalytic pathways involving transition-metal oxides and bifunctional solids have shown potential for glucose conversion. However, most investigations remain limited to the isomerization–dehydration sequence without completing the whole oxidation route to FDCA. Hierarchical zeolites, particularly ZSM-5, offer enhanced pore accessibility, tunable acidity, and thermal stability (Pratama et al., 2020b). At the same time, incorporating redox-active metals such as NiO may facilitate glucose dehydrogenation and the oxidation of furanic intermediates (Tanjung et al., 2025). Moreover, the use of γ-valerolactone–water mixtures has emerged as a critical factor in enhancing glucose conversion pathways, as this solvent system improves substrate solubility, stabilizes reactive intermediates, and promotes selective oxidation toward FDCA

(Al Ghatta et al., 2021; Kim et al., 2020). However, the combined influence of hierarchical pore architecture, metal dispersion, solvent effects, and reaction temperature on FDCA formation has not been systematically explored. Existing research rarely integrates these factors within a one-pot catalytic system, leaving a gap in optimization of metal-modified hierarchical zeolites for efficient glucose-to-FDCA conversion.

From a theoretical perspective, the integration of acidic zeolitic frameworks with redox-active metal oxides can be interpreted through the concept of bifunctional catalysis, where spatial proximity between Brønsted acid sites and redox centers enables sequential dehydration–oxidation pathways (Jiang et al., 2019; Tanjung et al., 2025). In hierarchical zeolite systems, the interplay between intrinsic reaction kinetics and mass transport phenomena further governs catalytic performance, as enhanced mesoporosity mitigates diffusion limitations and improves access of bulky intermediates to active sites (Ramadhani et al., 2022; Sabarish & Unnikrishnan, 2017). Moreover, selective HMF oxidation over transition-metal catalysts has been widely discussed in terms of structure–activity relationships and redox site functionality (Liu et al., 2024). Nevertheless, uncertainties remain regarding the dominant mechanistic pathway in glucose-to-FDCA conversion, particularly in distinguishing hydride-shift and enediol mechanisms (Marianou et al., 2016), as well as the extent to which solvent composition and reaction temperature modulate intermediate stabilization and oxidation steps in one-pot systems (Almhofer et al., 2023; Zhou et al., 2017).

To address these limitations, this study aims to evaluate the catalytic performance of NiO-modified hierarchical ZSM-5 and compare it with the parent ZSM-5 and NiO catalysts in the one-pot conversion of glucose to FDCA. This study applies a head-to-head benchmarking approach under identical reaction conditions to systematically evaluate the catalytic performance of hierarchical ZSM-5, NiO-modified ZSM-5, and bulk NiO, thereby enabling an assessment of structure–performance relationships in the one-pot conversion of glucose to FDCA. Systematic optimization of key reaction parameters, including temperature and the γ-valerolactone (GVL)–water solvent ratio, is carried out to determine their roles in enhancing FDCA yield. Through comprehensive physicochemical characterization of the catalysts, this work seeks to elucidate the synergistic relationships between the metal species integrated within the zeolitic framework and to analyze their catalytic behavior, while establishing critical design principles regarding the influence of temperature and solvent ratios for the efficient conversion of glucose to FDCA.

2. Methods

2.1 Materials

All reagents and chemicals involved in this study, including deionized water, conformed to analytical-grade standards and were employed without further purification unless otherwise stated. Nickel(II) nitrate hexahydrate ($Ni(NO_3)_2{\cdot}6H_2O$, analytical grade), tetrapropylammonium hydroxide (TPAOH, 40 wt.%), sodium aluminate ($NaAlO_2$), tetraethyl orthosilicate (TEOS, 98%), and poly(diallyldimethylammonium) chloride (PDDA-Cl, 20 wt.%) were purchased from Sigma Aldrich. γ-valerolactone (GVL, 99 %), methanol (CH_3OH, LC-grade), 2,5-furandicarboxylic acid (FDCA, 97 %, analytical grade, Merck), hydrogen peroxide (H_2O_2, 30 %, analytical grade), and potassium carbonate (K_2CO_3, ≥99 %, analytical grade were acquired from Merck.

2.2 Preparation of Hierarchical ZSM-5 Zeolite Synthesized, Hierarchical NiO/ZSM-5 Zeolite, and NiO

The synthesis of hierarchical ZSM-5 was conducted according to the method reported by Nurani et al. (2018), employing a dual-template strategy in which $NaAlO_2$ and TEOS served as the aluminum and silicon precursors, respectively, while TPAOH and PDDA-Cl (20 wt%) served as the main and secondary structure-directing agents, respectively.

Hydrothermal crystallization was performed at 150 °C for 6 days. Afterward, the solid was recovered by filtration and then calcined at 550 °C for 5 h to eliminate the organic templates. The resulting material was subsequently examined by x-ray diffraction (XRD), fourier transform infrared spectroscopy (FT-IR), nitrogen adsorption–desorption isotherms using Brunauer–Emmett–Teller (BET) surface analysis, and scanning electron microscopy coupled with energy-dispersive X-ray spectroscopy (SEM-EDS).

Metal oxides were incorporated into ZSM-5 via an impregnation–spray technique. The metal precursor was prepared by dissolving $Ni(NO_3)_2{\cdot}6H_2O$ in water, and the required amounts were determined to achieve a final metal loading of 10% on the ZSM-5 support. The resulting solution was added incrementally to the ZSM-5 crystals while stirring, then dried under ambient conditions. The dried solids were subsequently calcined at 550 °C for 5 hours under ambient pressure to generate the metal oxide–modified zeolite. Nickel oxide was prepared via an alkaline precipitation route (Bahari Molla Mahaleh et al., 2008; Deekala et al., 2020). $Ni(NO_3)_2{\cdot}6H_2O$ was dissolved in deionized water to form a homogeneous solution, then adjusted to pH 11 with 1 M NaOH under continuous mixing. The resulting mixture was then aged for 24 hours until a solid phase was formed. The precipitate was separated, washed using deionized water, oven-dried at 110 °C for 2 hours, and subsequently calcined at 450 °C for 1.5 hours to obtain NiO.

2.3 Characterization method

Following synthesis, all catalysts were thoroughly characterized to verify successful preparation and to examine their structural, elemental composition, and textural properties. The crystalline framework of the parent and metal-modified ZSM-5 samples was analyzed using a PANalytical Empyrean X-ray diffractometer operated at 40 kV and 30 mA with Cu Kα radiation over the 2θ range of 5–70°. Functional groups and framework vibrations were identified by Fourier Transform Infrared (FTIR) spectroscopy using the KBr pellet method at a resolution of 4 cm^{-1}. Textural properties were determined from N_2 adsorption–desorption measurements at 77 K on a Quantachrome Quadrasorb-Evo system, with samples pretreated by degassing at 300 °C before analysis; specific surface area was calculated using the BET method. The pore size distribution was calculated using the non-local density functional theory (NLDFT) model, based on nitrogen adsorption isotherm data from the instrument software. Surface morphology and metal dispersion were examined using SEM-EDX.

2.4 Catalytic test

The glucose-to-FDCA conversion was conducted based on a modified protocol derived from the method previously reported by Herlina et al. (2025). A reaction mixture containing D-glucose and the NiO/ZSM-5 catalyst at a 10:1 (w/w) ratio was prepared in 10 mL of a GVL–water solvent system with various compositions. The mixture was transferred to a glass vial, and temperature control was maintained using an oil bath with continuous stirring at the designated temperature for 4 hours. Hydrogen peroxide was then introduced as the oxidant, along with K_2CO_3 to establish a basic environment and facilitate FDCA dissolution, and the reaction was continued for a further 4 hours. After a total reaction time of 8 hours, the vial was immersed in a cold-water bath to quench the reaction effectively. The selected temperature range and solvent compositions were chosen based on literature benchmarks and preliminary screening to establish comparative performance trends rather than to conduct exhaustive parametric optimization. The resulting suspension was filtered to separate the catalyst, and the liquid phase was collected for further analysis. All catalytic experiments were performed in duplicate, and the reported values represent the average of two independent runs.

Quantitative analysis of FDCA was carried out using a PG LC210 high-performance liquid chromatography (HPLC) system equipped with a reversed-phase C18 column and a UV detector. Chromatographic separation was achieved using a mobile phase composed of

5 mM aqueous H_2SO_4 and methanol at a 9:1 volumetric ratio, operated at a constant flow rate of 1.0 mL min^{-1} (Herlina et al., 2025). The column temperature was maintained at 25 °C. Calibration curves were constructed using FDCA standard solutions to ensure accurate quantification. The FDCA yield (wt%) was calculated according to the following equation:

$$\%yield\ of\ FDCA = \frac{total\ concentration\ (\frac{mg}{L}) \times solution\ volume\ (L)}{glucose\ mass\ (mg)} \quad \text{(Eq. 1)}$$

3. Results and Discussion

3.1 Catalyst characterizations

X-ray diffraction analysis was employed to investigate the crystallinity and structural features of the synthesized catalysts, as illustrated in Fig. 1a. The hierarchical ZSM-5 sample exhibits the typical reflections of the MFI topology, with well-resolved peaks in the 2θ regions of 7–10° and 22–25°. These features match the reference pattern of ZSM-5 (ICDD 00-044-0003), confirming that the synthesis successfully produced a well-ordered MFI framework (Park et al., 2022). The absence of additional reflections indicates that no secondary phases or crystalline impurities formed during the hierarchical synthesis route, consistent with observations in previous hierarchical ZSM-5 studies (Pratama et al., 2020a).

After NiO impregnation, all dominant MFI reflections are preserved, confirming successful incorporation of metal species without compromising the integrity of the zeolite framework. In addition to the ZSM-5 peaks, several new reflections emerge at higher 2θ values, corresponding to NiO. These reflections confirm the successful integration of crystalline NiO species on the external regions of the zeolite framework, consistent with previously reported NiO/ZSM-5 systems (Tanjung et al., 2025). The presence of distinct NiO peaks indicates that the metal oxide is predominantly present as segregated crystalline particles rather than as highly dispersed ionic species within the zeolite framework.

Compared to the parent zeolite, the NiO/ZSM-5 diffractogram retains all major reflections of the MFI framework, confirming that the impregnation process did not significantly affect the structural integrity of the material. The appearance of additional peaks corresponding to NiO confirms that crystalline NiO phases were successfully deposited on the ZSM-5 surface without disrupting the integrity of the zeolite framework. This NiO/ZSM-5 prepared material demonstrates that modification of the impregnation–spray technique produced a composite material with a stable MFI structure and clearly identifiable nickel oxide species, as evidenced by the XRD pattern.

The diffractogram of the NiO reference material displays sharp, intense reflections typical of highly crystalline NiO, with peaks at approximately 2θ = 37.2°, 43.3°, 62.9°, 75.5°, and 79.1°. These positions correspond to the characteristic lattice planes of cubic NiO (JCPDS 78-0643) (Kumar & Das, 2021). The strong agreement between these reflections and those observed in the NiO/ZSM-5 sample further validates that the supported NiO retains its crystalline nature upon deposition. Overall, the XRD analysis confirms three key findings: hierarchical ZSM-5 was successfully synthesized, the MFI-type framework is preserved following NiO incorporation, and crystalline NiO species are effectively deposited on the zeolite surface.

The FTIR spectra of the synthesized ZSM-5, NiO/ZSM-5, and NiO materials are presented in Fig. 1b. The parent ZSM-5 exhibits the characteristic vibrational bands associated with the aluminosilicate MFI framework. The intense absorption features in the region of 1250–950 cm^{-1} are attributed to the asymmetric stretching modes of T–O–T bonds, where T represents Si or Al, while the bands within 800–700 cm^{-1} arise from the symmetric stretching modes of the tetrahedral framework units. In addition, the peak near 550 cm^{-1}, attributable to the double five-membered ring (D5R) units that typify the pentasil structure, further confirms the successful formation of the MFI topology, consistent with previous studies (Kostyniuk et al., 2020).

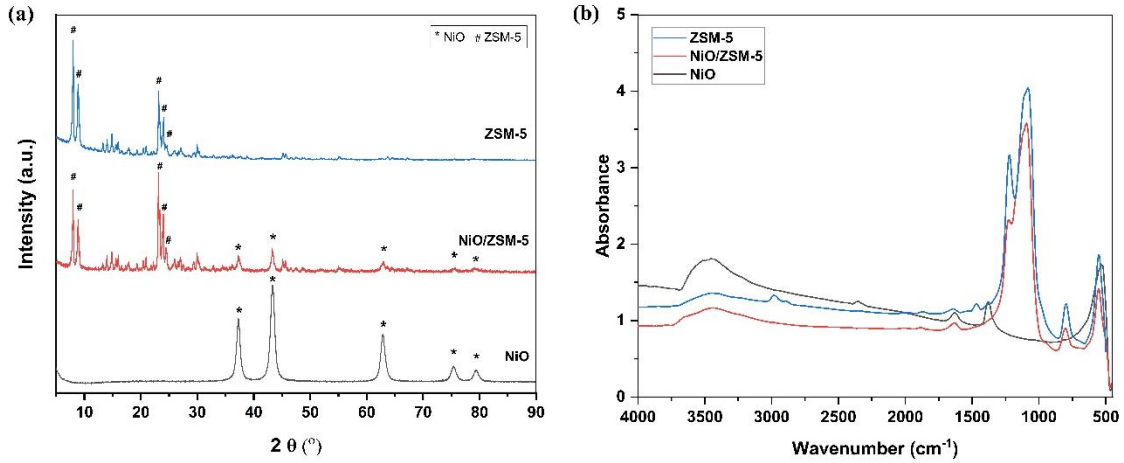

Fig. 1. (a) XRD patterns; (b) FTIR spectra of the as-synthesized and modified catalysts

Vibrations associated with the surface of hydroxyl groups appear in the broad absorption region of 3600–3200 cm^{-1}, which is commonly attributed to hydrogen-bonded silanol (Si–OH) groups and adsorbed water molecules. A weaker band near 1620 cm^{-1} corresponds to the vibrational bending mode corresponding to H–O–H, also indicative of physisorbed water. The overall hydroxyl features observed in the ZSM-5 spectrum align well with typical hierarchical or partially open-framework aluminosilicates reported in the literature.

Following NiO deposition, the NiO/ZSM-5 spectrum retains all the major bands characteristic of the MFI framework, which confirms that the metal oxide incorporation process does not disrupt the structural integrity of the zeolite lattice. Slight differences in band intensity are observed in the O–H stretching region. The slightly lower absorbance in the 3600–3200 cm^{-1} region suggests partial interaction between NiO species and surface silanol groups, analogous to effects reported for other metal-oxide-modified ZSM-5 systems (Asghar et al., 2020). This interaction may arise from surface anchoring of NiO particles, which reduces the amount of free hydrogen-bonded silanols.

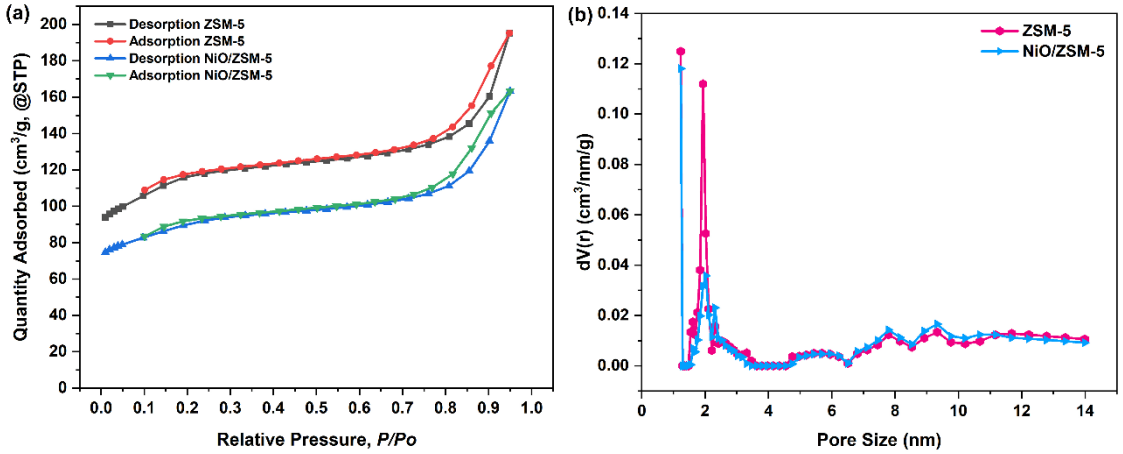

Fig. 2. Nitrogen physisorption analysis showing (a) adsorption–desorption isotherms; (b) pore size distributions for ZSM-5 and NiO/ZSM-5

Additional features in the fingerprint region provide evidence of NiO. The NiO sample exhibits broad metal–oxygen vibrational bands in the low-wavenumber region (600–400 cm^{-1}), consistent with Ni–O lattice modes reported for crystalline NiO (Kumar & Das, 2021). In the NiO/ZSM-5 spectrum, subtle shoulders and broadening within this region can be observed, indicating the coexistence of Ni–O species with the underlying zeolite framework vibrations. Although these Ni–O bands partially overlap with the intrinsic pentasil double-

ring band near 550 cm^{-1}, the changes in peak shape and relative intensity compared with the parent ZSM-5 further support the successful deposition of metal oxide species.

Overall, the FTIR results confirm that the MFI framework of ZSM-5 remains intact after NiO incorporation, as indicated by the preservation of all characteristic aluminosilicate vibrational bands. Minor shifts in the O–H stretching region suggest interactions between NiO and surface silanol groups, while the appearance of Ni–O vibrations in the fingerprint region further verifies the presence of supported metal oxide species. These spectral features are entirely consistent with the XRD observations, collectively demonstrating that the characterization results substantiate the successful construction of hierarchical ZSM-5 and the effective anchoring of NiO species on the zeolite surface.

As shown in Fig. 2a, BET nitrogen physisorption measurements for ZSM-5 and NiO/ZSM-5 reveal type IV isotherms accompanied by an H4 hysteresis loop in the mid-pressure region, evidencing the coexistence of micro- and mesoporous domains in the hierarchical zeolite framework. This profile is consistent with mesostructured ZSM-5 produced via soft-templating routes and aligns with previous reports on hierarchical MFI zeolites (Che et al., 2019). The higher nitrogen uptake of the parent ZSM-5 across the entire P/P_0 range reflects greater accessible porosity relative to its NiO-modified counterpart.

The quantitative textural parameters listed in Table 1 indicate that ZSM-5 has a high BET surface area (368 $m^2\ g^{-1}$), dominated by microporosity (273 $m^2\ g^{-1}$), with an external surface area of 95 $m^2\ g^{-1}$. After NiO introduction, S_{BET} decreases to 290 $m^2\ g^{-1}$, and Smicro drops significantly to 172 $m^2\ g^{-1}$, while Sexternal increases to 118 $m^2\ g^{-1}$. This behavior indicates partial blockage of micropores by NiO species, accompanied by the formation of additional surface-accessible NiO on the external or mesopore regions. Such trends are characteristic of metal-loaded ZSM-5 catalysts, in which metal oxide clusters exceed the intrinsic micropore dimensions and accumulate near pore mouths or on the outer surfaces (Che et al., 2019; Ramadhani et al., 2022).

Changes in pore volume further support this interpretation. The overall pore volume is reduced from 0.30 to 0.25 $cm^3\ g^{-1}$ after NiO addition, mainly due to a reduction in mesopore volume (0.21 to 0.13 $cm^3\ g^{-1}$), consistent with the lower N_2 uptake at intermediate P/P_0. Meanwhile, Vmicro increases slightly from 0.09 to 0.12 $cm^3\ g^{-1}$, likely arising from localized adjustments in pore accessibility or minor pore widening, a phenomenon occasionally observed in hierarchical materials following metal deposition. DFT pore size distributions (Fig. 2b) further confirm the retention of characteristic micropore (~1.2 nm) and mesopore (~2.02 nm) diameters, indicating that NiO deposition does not disturb the hierarchical pore architecture. The stability of pore dimensions aligns with reports that hierarchical ZSM-5 textural properties retain their micro–mesoporous network even after incorporation of metal oxides (Kim et al., 2012; Ramadhani et al., 2022).

Table 1. Summary of physicochemical parameters of ZSM-5 and NiO/ZSM-5

Catalyst	Nitrogen-physisorption								EDS (%wt)	
	[a]S_{BET} (m^2/g)	[a]S_{micro} (m^2/g)	[a]S_{ext} (m^2/g)	[c]V_{total} (cm^3/g)	[b]V_{micro} (cm^3/g)	[b]V_{ext} (cm^3/g)	[d]Pore Diameter (nm)		Si/Al ratio	Ni
ZSM-5	368	273	95	0.30	0.09	0.21	1.20	2.02	32.6	-
NiO/ZSM-5	290	172	118	0.25	0.12	0.13	1.20	2.02	27.7	10.1

Overall, the nitrogen physisorption results verify the successful synthesis of hierarchical ZSM-5 with well-preserved micro–mesoporous connectivity. NiO incorporation decreases surface area and mesopore accessibility due to partial pore obstruction, yet maintains the textural integrity of the hierarchical network. These textural features provide a favorable environment for biomass conversion, where mesopores facilitate diffusion of bulky reactants, micropores give stability, and NiO species contribute accessible active sites for oxidation and reforming pathways.

The surface morphological features of the hierarchical ZSM-5 and NiO/ZSM-5 catalysts were analyzed using scanning electron microscopy (SEM), as illustrated in Fig. 3. The parent ZSM-5 (Fig.3a) exhibits well-defined coffin-shaped hexagonal crystals characteristic of the MFI topology, consistent with previous reports describing TPAOH-templated ZSM-5

textures (Herlina et al., 2024; Pratama et al., 2020b). The crystals display smooth external surfaces with no evidence of structural distortion, indicating successful formation of the hierarchical zeolite framework. After NiO impregnation, the overall crystal morphology remains intact, and no collapse or fragmentation of the MFI structure is observed, consistent with earlier findings on metal-loaded ZSM-5 (Ramadhani et al., 2022; Tanjung et al., 2025). However, NiO/ZSM-5 (Fig. 3b) exhibits noticeably rougher crystal surfaces and the appearance of fine granular features adhering to the zeolite exterior, which correspond to NiO deposits introduced during the impregnation–spray process.

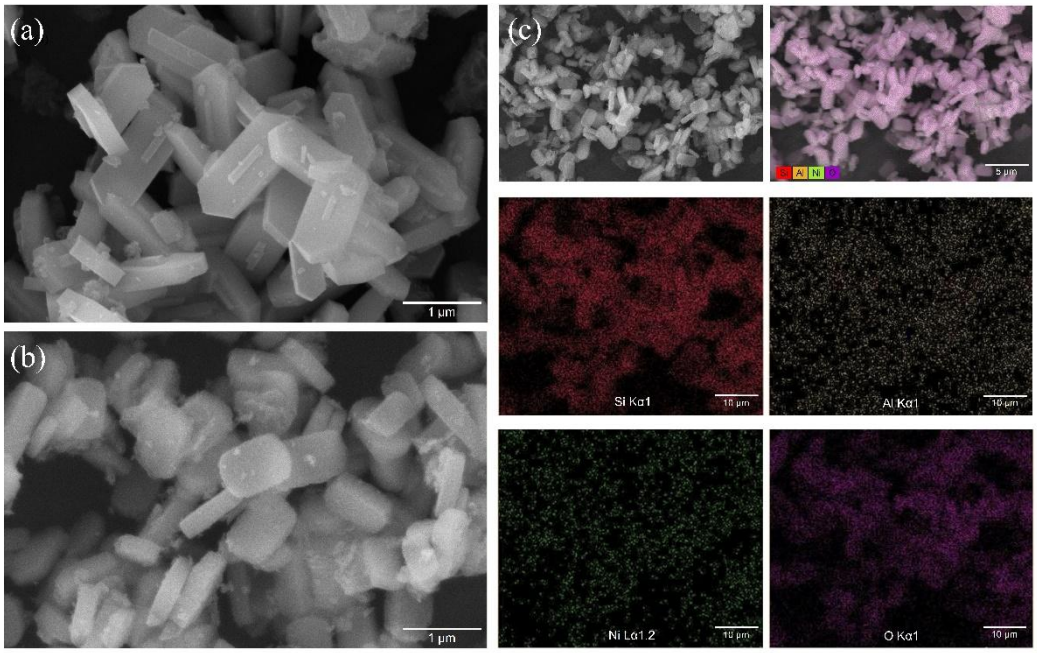

Fig. 3. Images of SEM characterization of (a) ZSM-5 and (b) NiO/ZSM-5, and (c) NiO/ZSM-5 EDS mapping

Elemental mapping provides further evidence of the successful incorporation and spatial distribution of the metal species (Fig. 3c). The EDS maps of Si, Al, O, and Ni reveal a homogeneous distribution of the framework elements and uniformly dispersed Ni throughout the crystal surfaces. Such uniformity is consistent with observations for Ni- and Co/Mo-modified ZSM-5 catalysts, in which metal oxides decorate the external surfaces without disrupting the underlying zeolite framework (Zhu et al., 2013). The uniform Ni signal also confirms that metal deposition occurs predominantly on surface-accessible sites, as is typical for hierarchical micro–mesoporous zeolites, which provide expanded external surfaces for metal anchoring. No localized agglomerates or intense hotspots of Ni are observed, indicating successful dispersion of the oxide phase and suggesting limited particle aggregation.

Quantitative EDS analysis (Table 1) further supports these observations. The parent ZSM-5 shows a high Si content (32.6 wt.%), consistent with the silica-rich hierarchical MFI framework. Following NiO incorporation, the Si and Al signals decrease (to 27.7 wt.% and corresponding Al levels), while Ni appears at 10.1 wt.%, reflecting successful metal loading. The reduction of Si and Al wt.% is attributed to surface coverage by NiO particles, which partially obscure the underlying framework elements in the probed region, a phenomenon also reported for MoO-, CoO-, CuO-, and NiO- modified ZSM-5 catalysts (Herlina et al., 2024; Prasad et al., 2023; Ramadhani et al., 2022). Together, the SEM and EDS analyses confirm that NiO species are effectively deposited on the hierarchical ZSM-5 surface, maintaining the intrinsic MFI crystal morphology while introducing well-dispersed active metal sites essential for subsequent catalytic reactions.

3.2 Catalytic test and optimization

The catalytic performance for glucose-to-2,5-furandicarboxylic acid conversion was assessed over parent hierarchical ZSM-5, hierarchical NiO/ZSM-5, and bulk NiO, alongside a non-catalytic reference experiment. The distinct crystalline phases identified by X-ray diffraction (ZSM-5, NiO/ZSM-5, and NiO) are expected to contribute differently to the overall catalytic behavior. In this study, D(+)-glucose was used as the substrate to assess the catalytic performance in FDCA production. Fundamentally, the catalytic transformation proceeds via a sequential reaction pathway, yielding FDCA as the final product. Several key intermediates are involved in this process, including fructose and 5-hydroxymethylfurfural, following the reaction sequence glucose → fructose → HMF → FDCA (Herlina et al., 2025).

From the perspective of glucose-to-FDCA conversion, which involves multiple sequential reaction steps, variations in catalyst composition and properties are expected to influence catalytic activity toward FDCA formation significantly. Accordingly, the initial stage of the discussion focuses on evaluating the catalytic performance of the three catalyst systems employed, namely parent hierarchical ZSM-5, hierarchical NiO/ZSM-5, and bulk NiO, in comparison with the non-catalytic reaction. The purpose of this evaluation is to select the catalyst demonstrating the highest performance before addressing the impact of other operational parameters. Figure 4a demonstrates that the uncatalyzed reaction produces only a minimal FDCA yield. In contrast, catalytic systems significantly promote the conversion of glucose into FDCA, with yields of 0.94% for ZSM-5, 2.36% for NiO/ZSM-5, and 0.58% for NiO.

When examining catalyst variation (Fig. 4a), it is evident that heterogeneous catalysts have a determining influence on reaction performance. Catalytic testing confirms that NiO/ZSM-5 significantly shows enhanced catalytic performance over pristine ZSM-5 and is markedly superior to bulk NiO, which is consistent with the structural, elemental composition, and textural properties of the catalysts revealed by the preceding characterization analyses. The catalyst promotes key reaction steps, including isomerization (Román-Leshkov et al., 2010), dehydration (Xu et al., 2025a), and oxidation (Herlina et al., 2024). The isomerization and dehydration processes are mainly catalyzed by acidic active sites (H^+) on the ZSM-5 surface, as evidenced by FTIR analysis showing characteristic Brønsted O–H silanol vibrations typical of ZSM-5 (Sabarish & Unnikrishnan, 2017), together with the Si/Al ratios obtained from EDS characterization, where a lower Si/Al ratio generally corresponds to a higher density of Brønsted acid sites (Li et al., 2022; Rahman et al., 2020), thereby accounting for the superior activity profile of the NiO/ZSM-5 catalyst. A detailed discussion on how the Si/Al ratio influences the acidity features of hierarchical ZSM-5 catalysts has been presented in our previous study (Ramadhani et al., 2022).

The catalytically active sites of ZSM-5 are essential in facilitating the glucose-to-fructose isomerization via multiple synergistic reaction pathways. This transformation proceeds via intramolecular hydride-shift mechanisms associated with the NiO/ZSM-5 framework, as well as C–C bond deprotonation and enediol intermediate formation pathways promoted by extra-framework NiO species (Tanjung et al., 2025). The isomerization process involves the initial glucose ring-opening step, followed by a molecular rearrangement that leads to fructose formation (Carraher et al., 2015), which is then acid-catalyzed to produce 5-hydroxymethylfurfural (HMF). The deposition of NiO on ZSM-5 via spray impregnation introduces additional redox-active centers, thereby enhancing the catalyst's bifunctional character. NiO species, dispersed on the external surface and inside the mesoporous network of ZSM-5, provide oxidative sites that activate H_2O_2 and facilitate electron transfer. Through these redox centers, the hydroxymethyl and aldehyde functionalities in HMF are selectively oxidized to carboxyl groups, resulting in 2,5-furandicarboxylic acid (FDCA) formation.

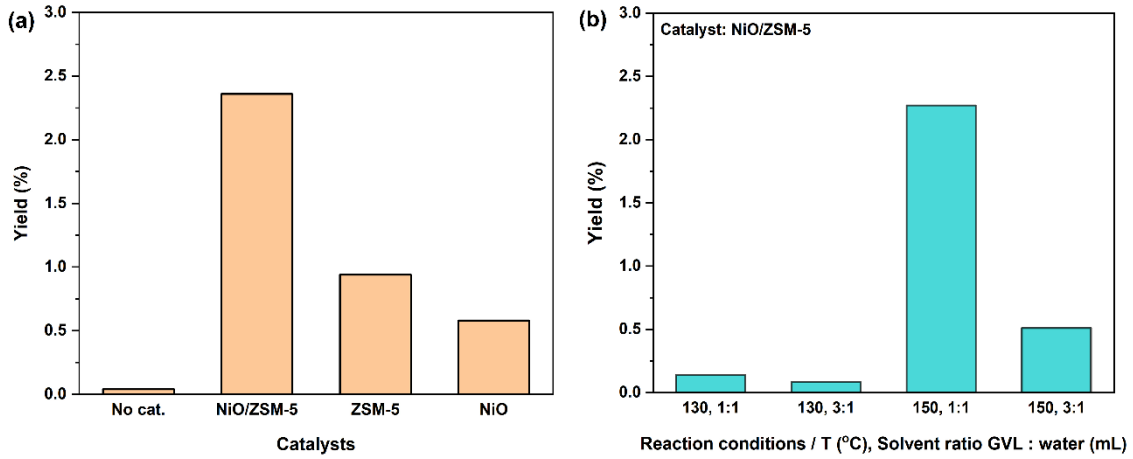

Fig. 4. Yield (%) of one-pot FDCA synthesis from glucose using (a) catalyst variation; (b) temperature and solvent ratio

The hierarchical architecture of ZSM-5, characterized by the coexistence of micro- and mesoporous networks, plays a critical role in enhancing the mass transport of bulky molecules such as glucose and its reaction products. This multiscale pore system alleviates diffusion limitations and facilitates efficient molecular access to active sites within the zeolite framework and to dispersed metal oxide species anchored on the catalyst surface. Consistent with the BET analysis, NiO/ZSM-5 shows a higher mesoporous surface area than the parent ZSM-5, which contributes to its superior catalytic performance. According to Teoh and Li (2012), NiO synthesized through a sol–gel method possesses a relatively low specific surface area in the range of 7.5–12.9 m^2 g^{-1} (Teoh & Li, 2012), which is a substantially lower value than ZSM-5 and NiO/ZSM-5. As a consequence, bulk NiO displays inferior catalytic performance compared to both ZSM-5 and NiO/ZSM-5. Overall, optimal conditions for glucose conversion to FDCA were achieved with NiO/ZSM-5, which demonstrated the best catalytic performance among the investigated systems.

After identifying the catalyst with the best performance, the effect of reaction temperature on glucose conversion and FDCA formation was investigated. Temperature variation was conducted to elucidate the influence of thermal conditions on substrate transformation, with reactions performed at 130 °C and 150 °C (Fig. 4b). Higher reaction temperatures led to greater product formation. This enhancement can be attributed to accelerated glucose dehydration to HMF at elevated temperature, followed by more efficient oxidation of furanic intermediates over the redox-active NiO sites, reflecting the synergistic interaction between the acidic framework of ZSM-5 and the incorporated NiO species. This observation is consistent with reports by T. Zhang et al. and Zhao et al., who demonstrated that temperatures above 150 °C promote glucose dehydration to HMF (Zhang et al., 2023; Zhao et al., 2023). These findings indicate that biomass-derived carbohydrate degradation requires elevated temperatures to promote reaction progression by mitigating the energy barrier (Chen et al., 2011). Elevating the reaction temperature also leads to higher liquid product yields by promoting faster sugar degradation and intensifying the overall reaction severity (Jeong et al., 2018). Moreover, higher operating temperatures impart greater kinetic energy to the reacting species, thereby increasing reaction rates (Herlina et al., 2024).

In addition to accelerating reaction rates, temperature critically influences the selectivity toward specific reaction products. At elevated temperatures, the formation of HMF and its subsequent oxidation to FDCA proceeds more efficiently. However, excessive temperature increases may promote undesired concurrent side processes, including furan ring opening and thermal decomposition, resulting in the formation of short-chain organic acids or humin byproducts (Almhofer et al., 2023; Sun et al., 2020; Xu et al., 2020). Therefore, selecting temperatures of 130 and 150 °C represents a compromise between providing sufficient thermal input to exceed the conversion barrier and maintaining the

oxidation pathway for product formation. In the investigated system, the presence of the NiO/ZSM-5 catalyst helps suppress the undesirable reaction pathway by stabilizing reaction intermediates at active, condensed sites within the zeolite framework. The synergy between the active sites of ZSM-5 and the redox sites of NiO enables controlled oxidation of HMF to FDCA, thereby maintaining product selectivity at higher reaction temperatures.

Beyond temperature, solvent selection decisively influences the feasibility of glucose transformation into FDCA. Accordingly, a solvent effect study was conducted using the optimal catalyst to elucidate its role in enhancing substrate solubility, stabilizing reaction intermediates, and suppressing the formation of byproducts. γ-Valerolactone (GVL) and water were used as solvents at two volume ratios, 1:1 and 3:1 (Fig. 4b). GVL is essential for stabilizing the HMF intermediate formed during the reaction. Moreover, the presence of GVL adjusts the solvent system polarity and mitigates HMF decomposition without inhibiting the dehydration step. In contrast, water facilitates the isomeric rearrangement of glucose to fructose through charged reaction routes and simultaneously promotes HMF degradation. These effects are in accordance with previous reports by J. Zhang et al. and Wu et al., which reported that water facilitates the solvation of H_2O_2 and supports electron-transfer reactions over transition-metal catalysts, whereas an increased GVL fraction stabilizes furanic intermediates and suppresses undesirable side reactions (Liu et al., 2024; Motagamwala et al., 2018).

In this study, the optimum conditions for glucose conversion to FDCA yielded a maximum FDCA formation of 2.27%, achieved under thermal conditions of 150 °C and at a specified solvent proportion of 1:1. This result aligns with Tanjung et al. (2025), who identified reaction temperature and its interaction with solvent volume as the dominant factors affecting product yield (Tanjung et al., 2025). Furthermore, increasing the GVL-to-water ratio to 3:1 was found to retard the reaction rate, which is in agreement with the findings reported by Herlina et al. (2025). The study found that the difference mainly stems from the solvent type: water accelerates the reaction, while GVL is more stable and environmentally friendly, though the reaction is slower (Herlina et al., 2025).

For the catalytic experiments, the total reaction time was fixed at 8 h, consisting of an initial 4 h during the isomerization and dehydration stages, after a subsequent 4 h oxidation stage upon addition of an oxidant (H_2O_2) and a basic salt (K_2CO_3). Hydrogen peroxide functions as an oxidizing agent to generate active oxygen species, while K_2CO_3 facilitates the formation of geminal diols and stabilizes the oxidation pathway, thereby promoting the formation of FDCA. According to the work of Herlina et al. (2025), the optimal reaction duration for D(+)-glucose conversion to FDCA was reported to be approximately 11 h based on a series of time-dependent experiments involving H_2O_2 and K_2CO_3 addition (Herlina et al., 2025). Nevertheless, several studies have demonstrated that glucose conversion to HMF typically requires about 4 h (Liang et al., 2019; Souzanchi et al., 2023; Zhou et al., 2017), while the subsequent oxidation of HMF to FDCA proceeds effectively within an additional 4 h (Albonetti et al., 2012; do Nascimento et al., 2024; Lei et al., 2017; Totaro et al., 2022). Accordingly, a total reaction time of 8 h was selected in this work to adequately accommodate both reaction stages.

In earlier research, one-pot glucose-to-FDCA systems have shown variable performance, depending on catalyst design and reaction conditions. Tanjung et al. reported an FDCA yield of 4.22% after process optimization, whereas Herlina et al. (2025) achieved 10–11.7% at 130 °C under extended reaction times of 9–25 h (Tanjung et al., 2025). More broadly, higher FDCA yields are often associated with two-step strategies involving separate HMF production followed by noble-metal-catalyzed oxidation (Davis et al., 2011; Motagamwala et al., 2018). Reviews emphasize that reported performance is strongly influenced by solvent system, oxidant selection, reactor configuration, and reaction severity (Sajid et al., 2018; Shen et al., 2024; Totaro et al., 2022). Recent studies integrating porous bifunctional solids with tailored redox functionality and solvent engineering highlight promising routes toward balancing catalytic efficiency and sustainability (Liang et al., 2019; Liu et al., 2024; Xu et al., 2025b). Within this landscape, the present study advances sustainable one-pot systems by systematically evaluating catalyst composition, hierarchical

structure, temperature, and solvent ratio in an earth-abundant bifunctional framework, providing mechanistic and structure–performance insights for rational catalyst design.

3.3 Proposed reaction mechanism

The conversion of D-glucose to 2,5-furandicarboxylic acid (FDCA) proceeds through a sequence of reaction steps catalyzed by metal-modified ZSM-5 systems (Fig. 5). The first stage involves glucose isomerization followed by dehydration to form 5-hydroxymethylfurfural (HMF). In the initial step, D-glucose molecules interact with the active sites on the catalyst surface, promoting isomerization to D-fructose via the formation of a 1,2-enediol intermediate (Herlina et al., 2025; Marianou et al., 2016). The presence of active metal species, such as NiO, is pivotal in stabilizing this intermediate and lowering the activation energy for proton and electron transfer during tautomerization (Ren et al., 2022; Tan et al., 2016; Ye et al., 2024). Subsequently, D-fructose undergoes stepwise dehydration, catalyzed through the active (silanol and Brønsted acid) sites of ZSM-5, yielding the furanic compound HMF. The hierarchical pore architecture of ZSM-5 enhances molecular diffusion and suppresses undesired side reactions, thereby favoring the selective dehydration of HMF from glucose.

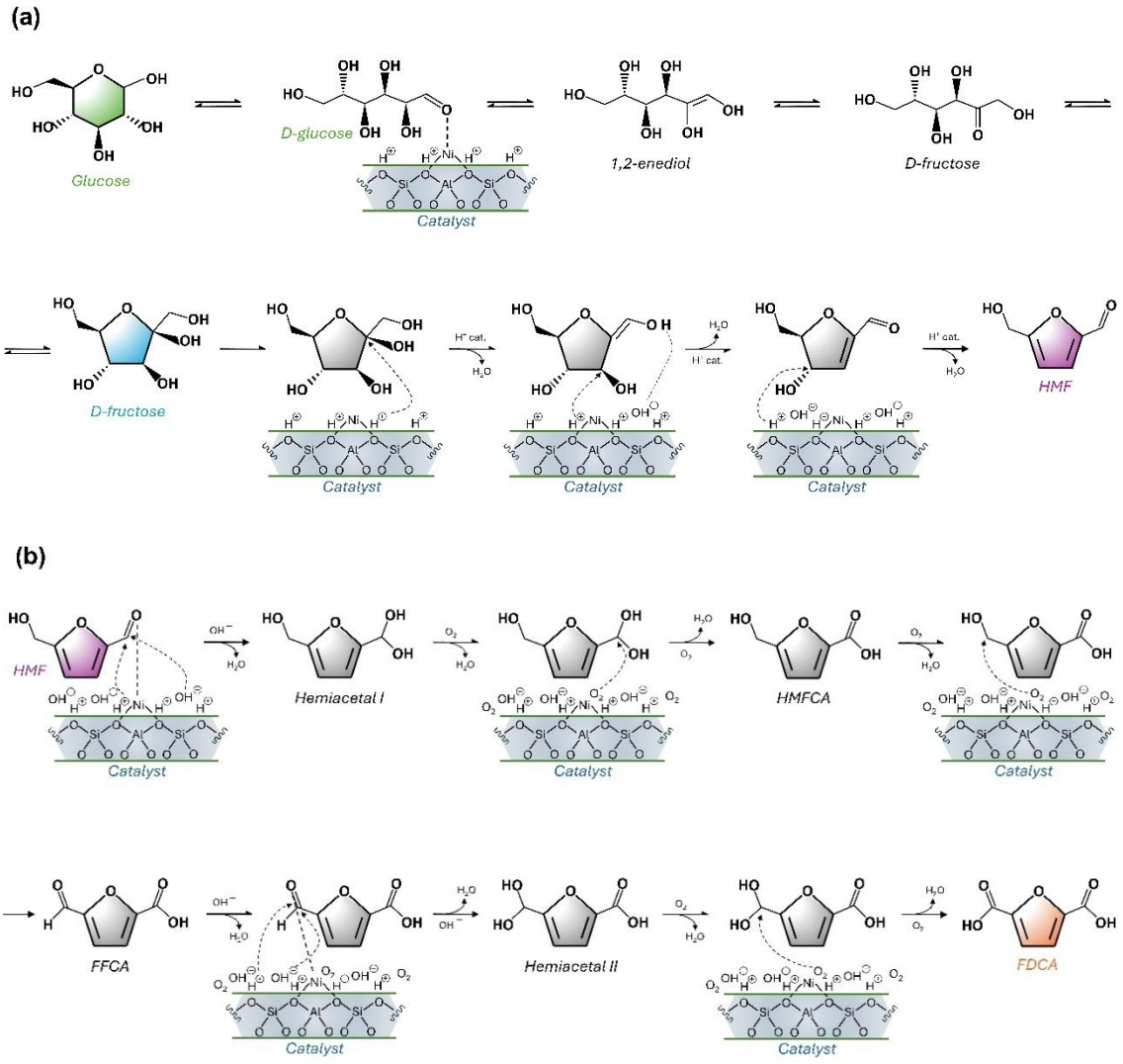

Fig. 5. Proposed reaction mechanism of glucose into FDCA

During the following oxidation step, oxidative conversion of HMF to FDCA is facilitated by hydrogen peroxide acting as the oxidizing agent, with K_2CO_3 added as a weak base to establish a moderately alkaline environment. This mild basicity helps stabilize HMF by preventing excessive pH elevation, thereby suppressing HMF degradation and minimizing the formation of undesired byproducts (Körner et al., 2019). In the initial oxidation step, the aldehyde functional group within the HMF molecule is adsorbed on the catalyst surface. In contrast, hydroxide ions derived from water are activated in the vicinity of the catalytic sites. This interaction triggers a reversible hydration reaction at the aldehyde group, which gives rise to a geminal diol intermediate (Herlina et al., 2025). The intermediate subsequently undergoes oxidative dehydrogenation to yield 5-hydroxymethyl-2-furancarboxylic acid (HMFCA), which desorbs from the surface of the catalyst (Bueno et al., 2026). In the following oxidation process, the hydroxymethyl group of HMFCA or the aldehyde group of 2,5-formylfurancarboxylic acid (FFCA) binds to the active sites of the catalyst, and it undergoes further oxidation (Tanjung et al., 2025). This process involves the formation of aldehyde and hemiacetal intermediates, which are ultimately oxidized to FDCA.

The integration of active sites inherent to the ZSM-5 framework with the redox functionality of NiO generates an effective synergistic system that directs the one-pot transformation of glucose to FDCA. The structural, elemental composition, and textural properties of the zeolite provide sites that promote glucose isomerization followed by dehydration to form HMF. In addition, the metal-oxide redox sites facilitate the selective oxidation of furanic intermediates without favoring degradation pathways. Moreover, the hierarchical pore architecture enhances molecular accessibility and diffusion while suppressing side-product formation, thereby enabling a more efficient and controlled reaction sequence. This cooperative catalytic behavior is consistent with the proposed mechanistic scheme illustrated in Fig. 5. It should be emphasized that ZSM-5 primarily provides acidic sites responsible for glucose isomerization and dehydration (Román-Leshkov et al., 2010), whereas NiO species function as redox-active centers for the subsequent oxidation steps (Liu et al., 2024; Tanjung et al., 2025), and the overall FDCA formation arises from their synergistic bifunctional interaction.

4. Conclusions

This study identifies that the principal contribution of hierarchical NiO/ZSM-5 zeolite catalysts in the one-pot conversion of glucose to 2,5-furandicarboxylic acid (FDCA) originates from their combined structural, elemental composition, and textural properties. Hierarchical H-ZSM-5 was successfully synthesized using a dual-template approach and subsequently modified via metal oxide impregnation employing a spray-assisted technique. Comprehensive catalyst characterization verified the successful synthesis and modification processes and demonstrated their close relationship with catalytic performance. X-ray diffraction results demonstrated that the retention of the characteristic crystalline framework of ZSM-5 was maintained after metal incorporation, ensuring structural integrity during the conversion process. Fourier-transform infrared spectroscopy identified key molecular features, particularly silanol groups characteristic of ZSM-5, which serve as Brønsted acid sites. Brunauer–Emmett–Teller analysis revealed that the hierarchical pore architecture enhanced reactant accessibility to active sites within the zeolite framework, while SEM–EDX analysis confirmed the structural, elemental composition, and textural properties, indicating that NiO species provide redox-active sites essential for oxidation reactions.

The hierarchical NiO/ZSM-5 catalyst exhibited the highest catalytic performance among the evaluated systems, achieving a maximum FDCA yield of 2.36% at 150 °C using a γ-valerolactone (GVL)/water solvent ratio of 1:1 after 4 h of reaction, followed by an additional 4 h upon the introduction of H_2O_2 and K_2CO_3 additives. This performance surpassed that of the parent zeolite and NiO bulk. Furthermore, the results demonstrate that reaction temperature and solvent ratio significantly influence FDCA yield. In general,

this study contributes significant insight into the design of bifunctional catalytic systems for the optimized one-pot transformation of glucose. It highlights the potential of FDCA as a key bio-derived intermediate for the manufacturing of polyethylene furanoate (PEF) and other renewable polyesters, positioning it as a promising sustainable alternative to fossil-based monomers. Although the present study establishes structural integrity and catalytic functionality, long-term durability and catalyst reusability require further investigation to fully assess practical applicability. Future studies should therefore focus on stability evaluation and potential deactivation mechanisms to further validate its role in sustainable biomass conversion.

Acknowledgement
We gratefully acknowledge the support of our institution, laboratory staff, and colleagues for their valuable assistance, technical guidance, and constructive discussions that contributed significantly to the completion of this research.

Author Contribution
Conceptualization, Y.K.K.; Methodology, Y.K.K. and R.W.; Validation, A.J.M. and A.P.P.; Formal Analysis, A.J.M.; Investigation, A.J.M. and A.P.P.; Data Curation, A.J.M. and A.P.P.; Writing – Original Draft Preparation, A.P.P.; Writing – Review & Editing, A.P.P. and Y.K.K.; Visualization, A.J.M. and A.P.P.; Supervision, Y.K.K. and R.W.; Project Administration, Y.K.K.; and Funding Acquisition, Y.K.K.

Funding
This research was supported by funding from the Ministry of Research and Higher Education, Republic of Indonesia, under research grant Hibah Dana Riset Pendidikan Magister Menuju Doktor untuk Sarjana Unggul (Hibah PMDSU) with grant contract number NKB-3040/UN2.R3.1/HKP.05.00/2019, and Universitas Indonesia, through the PUTI Q1 Grant Program, under grant number NKB-453/UN2.RST/HKP.05.00/2024.

Ethical Review Board Statement
Not available.

Informed Consent Statement
Not available.

Data Availability Statement
Not available.

Conflicts of Interest
The authors declare no conflict of interest.

Declaration of Generative AI Use
During the preparation of this work, the author(s) used a generative AI tool to assist in paraphrasing certain sections for clarity, Grammarly to assist in improving the grammar and academic tone of the manuscript, and generative AI tools for figure generation. After using these tools, the author(s) reviewed and edited the content as needed and took full responsibility for the content of the publication.

References

Al Ghatta, A., Wilton-Ely, J. D. E. T., & Hallett, J. P. (2021). From sugars to FDCA: a techno-economic assessment using a design concept based on solvent selection and carbon dioxide emissions. *Green Chemistry*, *23*(4), 1716–1733. https://doi.org/10.1039/d0gc03991h

Albonetti, S., Pasini, T., Lolli, A., Blosi, M., Piccinini, M., Dimitratos, N., Lopez-Sanchez, J. A., Morgan, D. J., Carley, A. F., Hutchings, G. J., & Cavani, F. (2012). Selective oxidation of 5-hydroxymethyl-2-furfural over TiO 2-supported gold-copper catalysts prepared from preformed nanoparticles: Effect of Au/Cu ratio. *Catalysis Today*, *195*(1), 120–126. https://doi.org/10.1016/j.cattod.2012.05.039

Almhofer, L., Bischof, R. H., Madera, M., & Paulik, C. (2023). Kinetic and mechanistic aspects of furfural degradation in biorefineries. *The Canadian Journal of Chemical Engineering*, *101*(4), 2033–2049. https://doi.org/10.1002/cjce.24593

Asghar, A., Iqbal, N., Aftab, L., Noor, T., Kariuki, B. M., Kidwell, L., & Easun, T. L. (2020). Ethylenediamine loading into a manganese-based metal-organic framework enhances water stability and carbon dioxide uptake of the framework. *Royal Society Open Science*, *7*(3). https://doi.org/10.1098/rsos.191934

Bahari Molla Mahaleh, Y., Sadrnezhaad, S. K., & Hosseini, D. (2008). NiO nanoparticles synthesis by chemical precipitation and effect of applied surfactant on distribution of particle size. *Journal of Nanomaterials*, *2008*(1), 4–7. https://doi.org/10.1155/2008/470595

Bosch, M., & Hazen, S. P. (2013). Lignocellulosic feedstocks: Research progress and challenges in optimizing biomass quality and yield. *Frontiers in Plant Science*, *4*(NOV), 1–3. https://doi.org/10.3389/fpls.2013.00474

Bueno, A., Viar, N., Conway, M. B., Gandarias, I., Requies, J. M., & Sankar, M. (2026). Aerobic oxidation of 5-Hydroxymethylfurfural to 2,5-Furandicarboxylic acid over Au/Hydrotalcite catalyst – role of support and synthesis methodology on the activity and stability. *Fuel*, *403*(April 2025), 136088. https://doi.org/10.1016/j.fuel.2025.136088

Carraher, J. M., Fleitman, C. N., & Tessonnier, J. P. (2015). Kinetic and mechanistic study of glucose isomerization using homogeneous organic brønsted base catalysts in water. *ACS Catalysis*, *5*(6), 3162–3173. https://doi.org/10.1021/acscatal.5b00316

Che, Q., Yang, M., Wang, X., Yang, Q., Rose Williams, L., Yang, H., Zou, J., Zeng, K., Zhu, Y., Chen, Y., & Chen, H. (2019). Influence of physicochemical properties of metal modified ZSM-5 catalyst on benzene, toluene and xylene production from biomass catalytic pyrolysis. *Bioresource Technology*, *278*, 248–254. https://doi.org/10.1016/j.biortech.2019.01.081

Chen, B., Abe, Y., Guo, H., & Lee Smith, R. (2024). Selective oxidation of 5-hydroxymethylfurfural over MnOx-CeO2 catalyst prepared with co-precipitation method. *Fuel*, *376*(July), 132745. https://doi.org/10.1016/j.fuel.2024.132745

Chen, Y., Li, G., Yang, F., & Zhang, S. (2011). Mn/ZSM-5 participation in the degradation of cellulose under phosphoric acid media. *Polymer Degradation and Stability*, *96*(5), 863–869. https://doi.org/10.1016/j.polymdegradstab.2011.02.007

Chioatto, E., Mancinelli, S., Mazzanti, M., & Onofrio, F. (2024). The Chemical sector in transition: Technological developments and green skills towards circularity and decarbonisation. *Current Opinion in Green and Sustainable Chemistry*, *50*, 100976. https://doi.org/10.1016/j.cogsc.2024.100976

Davis, S. E., Houk, L. R., Tamargo, E. C., Datye, A. K., & Davis, R. J. (2011). Oxidation of 5-hydroxymethylfurfural over supported Pt, Pd and Au catalysts. *Catalysis Today*, *160*(1),

55–60. https://doi.org/10.1016/j.cattod.2010.06.004
de Jong, E., Visser, H. A., Dias, A. S., Harvey, C., & Gruter, G. J. M. (2022). The Road to Bring FDCA and PEF to the Market. *Polymers*, *14*(5), 1–32. https://doi.org/10.3390/polym14050943
Deekala, V., Yazala, J. P., Sapavath, M., Kowthalam, A., & Rudraraju, R. (2020). Synthesis and Characterization of Nickel Oxide Nanoparticles Synthesized via Chemical Precipitation Method. *IOSR Journal of Applied Chemistry (IOSR-JAC)*, *2263*(10), 38–44. https://doi.org/10.1063/5.0016855
Deshan, A. D. K., Atanda, L., Moghaddam, L., Rackemann, D. W., Beltramini, J., & Doherty, W. O. S. (2020). Heterogeneous Catalytic Conversion of Sugars Into 2,5-Furandicarboxylic Acid. *Frontiers in Chemistry*, *8*(July), 1–23. https://doi.org/10.3389/fchem.2020.00659
do Nascimento, M. A., Haber, B., Gomez, M. R. B. P., Leao, R. A. C., Pietrowski, M., Zielinski, M., de Souza, R. O. M. A., Wojcieszak, R., & Itabaiana, I. (2024). Optimization of 5-hydroxymethylfurfural oxidation via photo-enzymatic cascade process. *Green Chemistry*, *26*(14), 8211–8219. https://doi.org/10.1039/d4gc00673a
Gong, W., Zheng, K., & Ji, P. (2017). Platinum deposited on cerium coordination polymer for catalytic oxidation of hydroxymethylfurfural producing 2,5-furandicarboxylic acid. *RSC Advances*, *7*(55), 34776–34782. https://doi.org/10.1039/c7ra05427k
Hayashi, E., Yamaguchi, Y., Kamata, K., Tsunoda, N., Kumagai, Y., Oba, F., & Hara, M. (2019). Effect of MnO2 Crystal Structure on Aerobic Oxidation of 5-Hydroxymethylfurfural to 2,5-Furandicarboxylic Acid. *Journal of the American Chemical Society*, *141*(2), 890–900. https://doi.org/10.1021/jacs.8b09917
Herlina, I., Krisnandi, Y. K., & Ridwan, M. (2024). Oxidation of 5-hydroxymethylfurfural into 2,5-furandicarboxylic acid over CuO and NiO modified natural sourced hierarchical ZSM-5. *South African Journal of Chemical Engineering*, *47*(December 2022), 75–82. https://doi.org/10.1016/j.sajce.2023.10.011
Herlina, I., Krisnandi, Y. K., & Ridwan, M. (2025). Production of 2,5-furandicarboxylic acid (FDCA) from delignified rice husk waste over Cu and Ni metal-organic framework catalyst. *Case Studies in Chemical and Environmental Engineering*, *11*(March), 101233. https://doi.org/10.1016/j.cscee.2025.101233
Jeong, H., Park, S., Ryu, G., Choi, J., Kim, J., & Choi, W. (2018). Catalytic conversion of hemicellulosic sugars derived from biomass to levulinic acid. *Catalysis Communications*, *117*(April), 19–25. https://doi.org/10.1016/j.catcom.2018.04.016
Jiang, L., Guo, H., Li, C., Zhou, P., & Zhang, Z. (2019). Selective cleavage of lignin and lignin model compounds without external hydrogen, catalyzed by heterogeneous nickel catalysts. *Chemical Science*, *10*(16), 4458–4468. https://doi.org/10.1039/c9sc00691e
Kim, H., Choi, J., & Won, W. (2020). Process synthesis and analysis of green plastic monomer production from cellulose. *Journal of Cleaner Production*, *277*, 124072. https://doi.org/10.1016/j.jclepro.2020.124072
Kim, Y. H., Lee, K. H., Nam, C.-M., & Lee, J. S. (2012). Formation of Hierarchical Pore Structures in Zn/ZSM-5 to Improve the Catalyst Stability in the Aromatization of Branched Olefins. *ChemCatChem*, *4*(8), 1143–1153. https://doi.org/10.1002/cctc.201200007
Körner, P., Jung, D., & Kruse, A. (2019). Influence of the pH Value on the Hydrothermal Degradation of Fructose. *ChemistryOpen*, *8*(8), 1121–1132. https://doi.org/10.1002/open.201900225
Kostyniuk, A., Key, D., & Mdleleni, M. (2020). 1-hexene isomerization over bimetallic M-Mo-ZSM-5 (M: Fe, Co, Ni) zeolite catalysts: Effects of transition metals addition on the catalytic performance. *Journal of the Energy Institute*, *93*(2), 552–564. https://doi.org/10.1016/j.joei.2019.06.009
Kumar, S., & Das, J. (2021). Synthesis, structural and magnetic properties of NiO nanospheres and rGO-NiO nanocomposites and observing magnetocaloric effect in rGO-NiO nanocomposites. *Materials Science and Engineering: B*, *265*(December 2020), 115007. https://doi.org/10.1016/j.mseb.2020.115007
Lei, D., Yu, K., Li, M. R., Wang, Y., Wang, Q., Liu, T., Liu, P., Lou, L. L., Wang, G., & Liu, S. (2017).

Facet Effect of Single-Crystalline Pd Nanocrystals for Aerobic Oxidation of 5-Hydroxymethyl-2-furfural. In *ACS Catalysis* (Vol. 7, Issue 1). https://doi.org/10.1021/acscatal.6b02839

Li, J., Gao, M., Yan, W., & Yu, J. (2022). Regulation of the Si/Al ratios and Al distributions of zeolites and their impact on properties. *Chemical Science*, *14*(8), 1935–1959. https://doi.org/10.1039/d2sc06010h

Liang, F., Chen, D., Liu, H., Liu, W., Xian, M., & Feng, D. (2019). One-Pot Synthesis of 5-Hydroxymethylfurfural from Glucose by Brønsted Acid-Free Bifunctional Porous Coordination Polymers in Water. *ACS Omega*, *4*(5), 9316–9323. https://doi.org/10.1021/acsomega.9b00882

Liu, J., Cheng, F., Zhou, S., Zhu, L., Xu, Q., Yin, D., & Liu, X. (2024). Efficient targeted acquisition 2,5-furandicarboxylic acid derived from 5-hydroxymethylfurfural over novel copper and vanadium oxide-functionalized catalysts. *Molecular Catalysis*, *560*(February), 114141. https://doi.org/10.1016/j.mcat.2024.114141

Marianou, A. A., Michailof, C. M., Pineda, A., Iliopoulou, E. F., Triantafyllidis, K. S., & Lappas, A. A. (2016). Glucose to Fructose Isomerization in Aqueous Media over Homogeneous and Heterogeneous Catalysts. *ChemCatChem*, *8*(6), 1100–1110. https://doi.org/10.1002/cctc.201501203

Motagamwala, A. H., Won, W., Sener, C., Alonso, D. M., Maravelias, C. T., & Dumesic, J. A. (2018). Toward biomass-derived renewable plastics: Production of 2,5-furandicarboxylic acid from fructose. *Science Advances*, *4*(1), 1–8. https://doi.org/10.1126/sciadv.aap9722

Nurani, D. A., Krisnandi, Y. K., & Akmal. (2018, September). Partial Oxidation of Methane Over NiOx/Hierachichal ZSM-5 Catalyst. In *Journal of Physics: Conference Series* (Vol. 1095, No. 1, p. 012005). IOP Publishing. https://doi.org/10.1088/1742-6596/1095/1/012005

Park, G., Kang, J., Park, S. J., Kim, Y. T., Kwak, G., & Kim, S. (2022). Effect of acid modification of ZSM-5 catalyst on performance and coke formation for methanol-to-hydrocarbon reaction. *Molecular Catalysis*, *531*(August), 112702. https://doi.org/10.1016/j.mcat.2022.112702

Prasad, K., Mahato, N., Yoo, K., & Kim, J. (2023). Morphology Regulated Hierarchical Rods-, Buds-, and Sheets-like CoMoO4 for Electrocatalytic Oxygen Evolution Reaction. *Energies*, *16*(5). https://doi.org/10.3390/en16052441

Pratama, A. P., Krisnandi, Y. K., & Abdullah, I. (2020a). Catalytic depolymerization of lignin from wood waste biomass over natural sourced ZSM-5 catalysts. *IOP Conference Series: Materials Science and Engineering*, *902*(1). https://doi.org/10.1088/1757-899X/902/1/012051

Pratama, A. P., Rahayu, D. U. C., & Krisnandi, Y. K. (2020b). Levulinic acid production from delignified rice husk waste over manganese catalysts: Heterogeneous versus homogeneous. *Catalysts*, *10*(3). https://doi.org/10.3390/catal10030327

Rahman, M., Infantes-Molina, A., Hoffman, A. S., Bare, S. R., Emerson, K. L., & Khatib, S. J. (2020). Effect of Si/Al ratio of ZSM-5 support on structure and activity of Mo species in methane dehydroaromatization. *Fuel*, *278*(May). https://doi.org/10.1016/j.fuel.2020.118290

Ramadhani, A. N., Abdullah, I., & Krisnandi, Y. K. (2022). Effect of Physicochemical Properties of Co and Mo Modified Natural Sourced Hierarchical ZSM-5 Zeolite Catalysts on Vanillin and Phenol Production from Diphenyl Ether. *Bulletin of Chemical Reaction Engineering & Catalysis*, *17*(1), 225–239. https://doi.org/10.9767/bcrec.17.1.13372.225-239

Rathod, P. V, & Jadhav, V. H. (2018). Efficient Method for Synthesis of 2,5-Furandicarboxylic Acid from 5-Hydroxymethylfurfural and Fructose Using Pd/CC Catalyst under Aqueous Conditions. *ACS Sustainable Chemistry & Engineering*, *6*(5), 5766–5771. https://doi.org/10.1021/acssuschemeng.7b03124

Ren, J., Cao, J. P., & Zhao, X. Y. (2022). Fabrication strategies of Ni-based catalysts in reforming of biomass tar/tar model compounds. *Applications in Energy and*

Combustion Science, *9*, 100053. https://doi.org/10.1016/j.jaecs.2021.100053

Román-Leshkov, Y., Moliner, M., Labinger, J. A., & Davis, M. E. (2010). Mechanism of glucose isomerization using a solid Lewis acid catalyst in water. *Angewandte Chemie (International Ed. in English)*, *49*(47), 8954–8957. https://doi.org/10.1002/anie.201004689

Sabarish, R., & Unnikrishnan, G. (2017). Synthesis, characterization and catalytic activity of hierarchical ZSM-5 templated by carboxymethyl cellulose. *Powder Technology*, *320*, 412–419. https://doi.org/10.1016/j.powtec.2017.07.041

Sajid, M., Zhao, X., & Liu, D. (2018). Production of 2,5-furandicarboxylic acid (FDCA) from 5-hydroxymethylfurfural (HMF): Recent progress focusing on the chemical-catalytic routes. *Green Chemistry*, *20*(24), 5427–5453. https://doi.org/10.1039/c8gc02680g

Shen, T., Hou, L., Gosset, J., Wang, H., Leng, S., Boumghar, Y., Barghi, S., & Xu, C. (2024). Recent advances in processes and technologies for production of 5-hydroxymethylfurfural and 2,5-furandicarboylic acid from carbohydrates. *Chemical Engineering Journal*, *500*(June). https://doi.org/10.1016/j.cej.2024.156470

Souzanchi, S., Nazari, L., Rao, K. T. V., Yuan, Z., Tan, Z., & Xu, C. (Charles). (2023). 5-HMF production from industrial grade sugar syrups derived from corn and wood using niobium phosphate catalyst in a biphasic continuous-flow tubular reactor. *Catalysis Today*, *407*(June 2021), 274–280. https://doi.org/10.1016/j.cattod.2021.07.032

Sun, C., Liao, Q., Xia, A., Fu, Q., Huang, Y., Zhu, X., Zhu, X., & Wang, Z. (2020). Degradation and transformation of furfural derivatives from hydrothermal pre-treated algae and lignocellulosic biomass during hydrogen fermentation. *Renewable and Sustainable Energy Reviews*, *131*(May), 109983. https://doi.org/10.1016/j.rser.2020.109983

Tan, M., Ma, L., Rehman, M. S. U., Ahmed, M. A., Sajid, M., Xu, X., Sun, Y., Cui, P., & Xu, J. (2019). Screening of acidic and alkaline pretreatments for walnut shell and corn stover biorefining using two way heterogeneity evaluation. *Renewable Energy*, *132*, 950–958. https://doi.org/10.1016/j.renene.2018.07.131

Tan, Z., Miao, G., Liu, C., Luo, H., Bao, L., Kong, L., & Sun, Y. (2016). Catalytic conversion of glucose into alkanediols over nickel-based catalysts: A mechanism study. *RSC Advances*, *6*(67), 62747–62753. https://doi.org/10.1039/c6ra14738k

Tanjung, M. F., Zulys, A., & Krisnandi, Y. K. (2025). Step-wise conversion of glucose into 2,5 furandicarboxylic acid (FDCA) in GVL-H2O solvent using hierarchical NiO/ZSM-5 catalyst. *Molecular Catalysis*, *586*(July), 115403. https://doi.org/10.1016/j.mcat.2025.115403

Teoh, L. G., & Li, K. D. (2012). Synthesis and characterization of NiO nanoparticles by solgel method. *Materials Transactions*, *53*(12), 2135–2140. https://doi.org/10.2320/matertrans.M2012244

Totaro, G., Sisti, L., Marchese, P., Colonna, M., Romano, A., Gioia, C., Vannini, M., & Celli, A. (2022). Current Advances in the Sustainable Conversion of 5-Hydroxymethylfurfural into 2,5-Furandicarboxylic Acid. *ChemSusChem*, *15*(13), 1–13. https://doi.org/10.1002/cssc.202200501

Wang, L., & Xiao, F. S. (2015). Nanoporous catalysts for biomass conversion. *Green Chemistry*, *17*(1), 24–39. https://doi.org/10.1039/c4gc01622j

Xu, C., Cai, J., Shi, W., Cui, L., & Wu, S. (2025a). Efficient synthesis of 2,5-furandicarboxylic acid from corncob biomass using Ru/C and sulfonated carbon catalysts in a one-pot system. *Biofuels, Bioproducts and Biorefining*, *19*(1), 109–120. https://doi.org/https://doi.org/10.1002/bbb.2696

Xu, H., Li, Q., Bi, Z., Xu, D., & Guo, Y. (2025b). Sustainable lactic acid production from glycerol via hydrothermal catalysis over highly dispersed cu nanoparticles on bio-tar derived carbon. *Journal of Environmental Chemical Engineering*, *13*(September). https://doi.org/10.1016/j.jece.2025.119275

Xu, Z., Yang, Y., Yan, P., Xia, Z., Liu, X., & Zhang, Z. C. (2020). Mechanistic understanding of humin formation in the conversion of glucose and fructose to 5-hydroxymethylfurfural in [BMIM]Cl ionic liquid. *RSC Advances*, *10*(57), 34732–34737. https://doi.org/10.1039/d0ra05641c

Ye, D., Wu, T., Puri, A., Hebert, D. D., Siegler, M. A., Hendrich, M. P., Swart, M., & Garcia-Bosch, I. (2024). Enhanced Proton-Coupled Electron-Transfer Reactivity by a Mononuclear Nickel(II) Hydroxide Radical Complex. *Inorganic Chemistry*, *63*(52), 24453–24465. https://doi.org/10.1021/acs.inorgchem.4c03370

Zhang, T., Wei, H., Jin, Y., & Xiao, H. (2023). Dehydration of glucose to 5-hydroxymethylfurfural over sn-containing dendritic mesoporous silica. *Chemical Engineering Journal*, *454*(P3), 140415. https://doi.org/10.1016/j.cej.2022.140415

Zhao, C., Zhu, N., Qiu, G., Zhang, M., & Tian, H. (2023). Effective Synergistic Hafnium-Aluminum Bimetallic Oxides catalysts for the Synthesis of 5-Hydroxymethylfurfural from Glucose and Fructose. *Molecular Catalysis*, *547*(May), 113407. https://doi.org/10.1016/j.mcat.2023.113407

Zhou, C., Zhao, J., Yagoub, A. E. G. A., Ma, H., Yu, X., Hu, J., Bao, X., & Liu, S. (2017). Conversion of glucose into 5-hydroxymethylfurfural in different solvents and catalysts: Reaction kinetics and mechanism. *Egyptian Journal of Petroleum*, *26*(2), 477–487. https://doi.org/10.1016/j.ejpe.2016.07.005

Zhu, Z., Lu, G., Zhang, Z., Guo, Y., Guo, Y., & Wang, Y. (2013). Highly Active and Stable Co3O4/ZSM-5 Catalyst for Propane Oxidation: Effect of the Preparation Method. *ACS Catalysis*, *3*(6), 1154–1164. https://doi.org/10.1021/cs400068v

Biographies of Authors

Arnia Putri Pratama, Department of Chemistry, Faculty of Mathematics and Natural Science, Universitas Indonesia, Depok, West Java 16424, Indonesia.

- Email: arnia.putri@sci.ui.ac.id
- ORCID: 0000-0003-1583-5257
- Web of Science ResearcherID: N/A
- Scopus Author ID: 58077997600
- Homepage: N/A

Andita Junia Mulyadi, Department of Chemistry, Faculty of Mathematics and Natural Science, Universitas Indonesia, Depok, West Java 16424, Indonesia.

- Email: andita.junia01@ui.ac.id
- ORCID: N/A
- Web of Science ResearcherID: N/A
- Scopus Author ID: N/A
- Homepage: N/A

Rahmat Wibowo, Department of Chemistry, Faculty of Mathematics and Natural Science, Universitas Indonesia, Depok, West Java 16424, Indonesia.

- Email: rahmat.wibowo@sci.ui.ac.id
- ORCID: 0000-0001-5431-4548
- Web of Science ResearcherID: N/A
- Scopus Author ID: 57200846522
- Homepage: https://scholar.ui.ac.id/en/persons/rahmat-wibowo/

Yuni Krisyuningsih Krisnandi, Department of Chemistry, Faculty of Mathematics and Natural Science, Universitas Indonesia, Depok, West Java 16424, Indonesia.

- Email: yuni.krisnandi@sci.ui.ac.id
- ORCID: 0000-0002-2753-5596
- Web of Science ResearcherID: AAD-9719-2019
- Scopus Author ID: 12761423100
- Homepage: https://scholar.ui.ac.id/en/persons/yuni-krisyuningsih